

# Low-temperature concentration of tellurium and gold in continental red bed successions

John Parnell,<sup>1</sup> Samuel Spinks<sup>1</sup> and David Bellis<sup>2</sup>

<sup>1</sup>School of Geosciences, University of Aberdeen, Aberdeen AB24 3UE, UK; <sup>2</sup>School of Natural and Computing Sciences, University of Aberdeen, Aberdeen AB24 3UE, UK

## ABSTRACT

There is very little understanding of tellurium (Te) distribution and behaviour in sedimentary rocks. A suite of 15 samples of reduction spheroids (centimetre-scale pale spheroids in otherwise red rock), including samples from eight localities in Triassic red beds across the British Isles, were mapped for Te using Laser Ablation–Inductively Coupled Plasma–Mass Spectrometry. Almost all showed enrichment in Te in the cores of the spheroids relative to background red bed concentrations, by up to four orders of magnitude. Some were also enriched over background in gold and/or mercury. In one case, discrete

telluride minerals were recorded. The data show that Te is mobile and can be concentrated in low-temperature sedimentary environments, controlled by redox variations. The consistency in enrichment across widely separate localities implies that the enrichment is a normal aspect of red bed diagenesis and so likely to be controlled by a ubiquitous process, such as microbial activity.

Terra Nova, 28: 221–227, 2016

## Introduction

The mobilization and concentration of gold (Au) are attributed particularly to high-temperature processes in magmatic, metamorphic and hydrothermal environments (Afifi *et al.*, 1988; Cook and Ciobanu, 2005). However, there is a growing recognition that reduction, commonly microbially mediated, can cause the solubilization and redistribution of Au and associated elements including tellurium (Te) at low temperatures. Tellurium is of increasing technological importance (Zweibel, 2010; Turner *et al.*, 2012; Zepf *et al.*, 2014) and is a critical metal for the development of low-carbon energy technologies in Europe (Moss *et al.*, 2011). In this study, we analyse reduction spheroids developed ubiquitously in red bed successions under possible microbial mediation, to test for Te enrichment, and find that almost all examples exhibit the concentration of Te over background levels by up to several orders of magnitude. Many similarly exhibit concentrations of mercury (Hg). Tellurium and Hg, among others, can be pathfinder elements for Au,

and in many cases, the spheroids are also enriched in Au.

Tellurium can fix Au within telluride minerals in Au ore deposits in a range of settings and can be a pathfinder element in Au exploration (Boyle, 1979; Ciobanu *et al.*, 2006). Conventionally, Au deposition is attributed to medium- to high-temperature environments, where Te is regarded as mobile and available (Afifi *et al.*, 1988; Cook and Ciobanu, 2005). By contrast, almost nothing is known about the behaviour of Te in sedimentary rocks, and except for some exceptional ocean floor deposits (Hein *et al.*, 2003), anomalous sedimentary concentrations of Te are unknown. Mercury concentrations in siliciclastic rocks are also extremely low (McNeal and Rose, 1974). Accordingly, Te and Hg are not known controls on Au distribution in sedimentary environments.

Gold mineralization can occur in or adjacent to continental red beds (red sandstones and mudrocks), implying the mobilization and fixing of Au by low-temperature processes (Shepherd *et al.*, 2005; Spinks *et al.*, 2016). To date, such deposits are exceptional and have been linked to anomalous Au availability through volcanic activity (Colman and Cooper, 2000). However, there is a growing recognition that reduction can cause the solubilization and redistribution of Au and other rare

metals at low temperatures (Shepherd *et al.*, 2005). This raises the possibility that there may be widespread mobility of Au in sediments with variable redox conditions, in contrast to its purported inert behaviour.

Continental red beds have a history back to the early Proterozoic, when sedimentation in oxidizing conditions first occurred. However, there were times when their occurrence was especially widespread, including the Mesoproterozoic, the Devonian (Old Red Sandstone) and the Permian–Triassic (New Red Sandstone). Red beds from each of these times contain abundant reduction spheroids, i.e. centimetre-scale pale spheroids in otherwise red rock, attributed a microbiological origin by many workers, and containing metal-rich cores (e.g. Harrison, 1975; Hofmann, 1990; Spinks *et al.*, 2010; Zhang *et al.*, 2014). This study assesses whether Te, Hg and Au become concentrated in these low-temperature red bed features, focusing on Triassic rocks that have never experienced high (>150 °C) temperatures.

## Material and methods

A set of 10 samples (eight localities, two duplicates to test consistency) of Triassic age over 900 km of the British Isles were analysed by laser ablation–inductively coupled plasma–mass spectrometry (LA-ICP-MS) to

Correspondence: John Parnell, School of Geosciences, University of Aberdeen, Aberdeen AB24 3UE, UK. Tel.: +44 1224 273464; fax: +44 1224 272785; e-mail: [j.parnell@abdn.ac.uk](mailto:j.parnell@abdn.ac.uk)

produce maps showing patterns of enrichment against background (Fig. 1). Samples were collected from bedding surfaces in mudrocks deposited in low-energy fluvial successions in the Upper Triassic Mercia Mudstone Group. For comparison, reduction spheroids of Mesoproterozoic age from Culkein, Scotland (Spinks *et al.*, 2010), Devonian age from Millport, Scotland (Spinks *et al.*, 2014), Carboniferous age from Car Rocks, Scotland and Cultra, Ireland, and Triassic age from Utah were treated in the same manner. Typically, rocks contained 50–100 spheroids  $\text{m}^{-3}$ . Samples were chosen with a core about 2 mm in diameter, suitable for seven or eight laser transects. Analysis was performed using a UP213 laser ablation (LA) system (New Wave) coupled to an Agilent 7500ce inductively coupled plasma–mass spectrometer (ICP-MS). LA-ICP-MS was tuned for maximum sensitivity and stability using standard SRM 612 for trace elements in glass (NIST), optimizing the energy fluence to about  $2 \text{ J/cm}^2$ . A semi-quantitative calibration was provided using MASS-1 Synthetic Polymetal Sulfide (USGS). Samples and the standard were analysed using a 100- $\mu\text{m}$  diameter round spot moving in a straight line at  $50 \mu\text{m s}^{-1}$ . A 15-s laser warm-up preceded 30 s of ablation (1.5 mm) and a 15-s delay.  $^{82}\text{Se}$  and  $^{125}\text{Te}$  were monitored for 0.1-s dwell time each. The average count signal from three lines over 20 s of the ablation was calculated for each element. The standard was used to calculate the concentration ( $\mu\text{g g}^{-1}$ )/counts ratio, which was multiplied by the sample counts to estimate the concentration. Bulk Te measurements were made on 2 cm-sized nodules from Budleigh, England, and Kirtomy, Scotland. The background (mudstone without spheroids) Te content for six occurrences was measured using solution ICP-MS. Spheroids from several localities in the Triassic of the East Midlands of England (Fig. 2) were studied using an ISI ABT-55 scanning electron microscope. Reduction spheroids in that region occur in the Mercia Mudstone Group, especially in the Cropwell Bishop Formation (Elliott, 1961). The four sites sampled in the East Midlands (Fauld,

Bantycok, Cropwell Bishop, Gipsy Lane) are all in active or former gypsum workings (Fig. 2), as are the sites in Ireland. In the East Midlands, Elliott (1961) noted that the spheroids in mudstones ‘may form local marker bands where they occur in profusion, as they do for instance in the roof of the ... gypsum mines’.

## Results

The LA-ICP-MS maps show Te enrichment in 9 of 10 Triassic samples (Fig. 1) by up to four orders of magnitude (Table 1), from background values of  $<1 \text{ p.p.m.}$  to maximum values commonly in the range  $10^3$ – $10^4 \text{ p.p.m.}$  Background values are all  $<0.1 \text{ p.p.m.}$ , consistent with previous measurements in sediments (Belzile and Chen, 2015). Whole core values of 2.4 and 4.5 p.p.m. (Table 1) confirm enrichment over background by orders of magnitude. Seven of 10 spheroids also show Hg, and all show some degree of Au enrichment, up to five orders of magnitude (Fig. 3). Comparison of data from multiple laser transects, and  $>100$  individual analyses, on each sample, which produce sensible maps (Fig. 3), was used to conclude that measurements were consistent and reliable. We emphasize the pattern of concentration at the cores, rather than the precise level of enrichment. Different elements show different enrichment patterns (Fig. 2), just as they are zoned variably in roll-front deposits, due to variable response to redox changes (Reynolds and Goldhaber, 1983). The degree of enrichment will vary between spheroids at the same locality, as demonstrated at Knocknacran and Bantycok (Fig. 1), but the significance of the dataset is that enrichment occurs consistently in widely separated localities. The samples of other ages also exhibit enrichment, giving us 15 examples in total (Table 1). Exceptionally, at Cropwell Bishop (Fig. 2), spheroid cores contain grains of a bismuth telluroselene (Fig. 4) with a composition referable to kawazulite (Kato, 1970). Maps prepared for Se did not show clear enrichment patterns in most cases. At Fauld, Bantycok, Gipsy Lane and Cropwell Bishop, selenide minerals (notably clausthalite) were detected by SEM

as abundant micron-scale grains in the spheroids, as they were in the Devonian spheroids from Millport (Spinks *et al.*, 2014).

## Discussion

### Conditions of concentration

The Triassic samples have never experienced temperatures exceeding  $100 \text{ }^\circ\text{C}$ . They have very shallow burial histories, typically no more than 2 km, and the maximum temperatures reached at two of the sites in central England and northwest Scotland are estimated at about  $80 \text{ }^\circ\text{C}$  (Kilenyi and Standley, 1985; McKinley *et al.*, 2012). At these near-surface temperatures and the high oxygen levels implied by red beds and neutral to alkaline conditions, Te oxyions predominate (McPhail, 1995), so Te should be mobile until it reaches a redox boundary, where it could become concentrated by progressive precipitation. The predominance of Te concentration over Se is consistent with the strongly oxidizing environment (Schirmer *et al.*, 2014).

The data (Figs 1, 3 and Table 1) show that there is consistent enrichment of Te, Hg and Au in the reduction spheroids, including spheroids from other geological periods. The degree of enrichment varies between spheroids, including between paired spheroids from a single locality, but enrichment occurs regardless of locality or age. The geological history of the samples chosen constrains the enrichment process to a low-temperature mechanism. The reduction features on which the enrichments are based are a widespread feature of modern-day buried sediment, in which most of the reduction in Fe(III) is caused by Fe(III)-reducing bacteria (Lovley, 1997), including thermophilic species that persist to deep burial. Where this bacterial activity is extensive, the red colour is stripped off sand grains and the sediment turns grey (Lovley, 1997); mottling of reduced and oxidized sediment develops, analogous to what is observed in the geological record, which is thus reasoned to reflect microbial activity (Lovley *et al.*, 1990). Fe(III)-reducing bacteria can reduce a range of other metals and metalloids, including V, Cu,

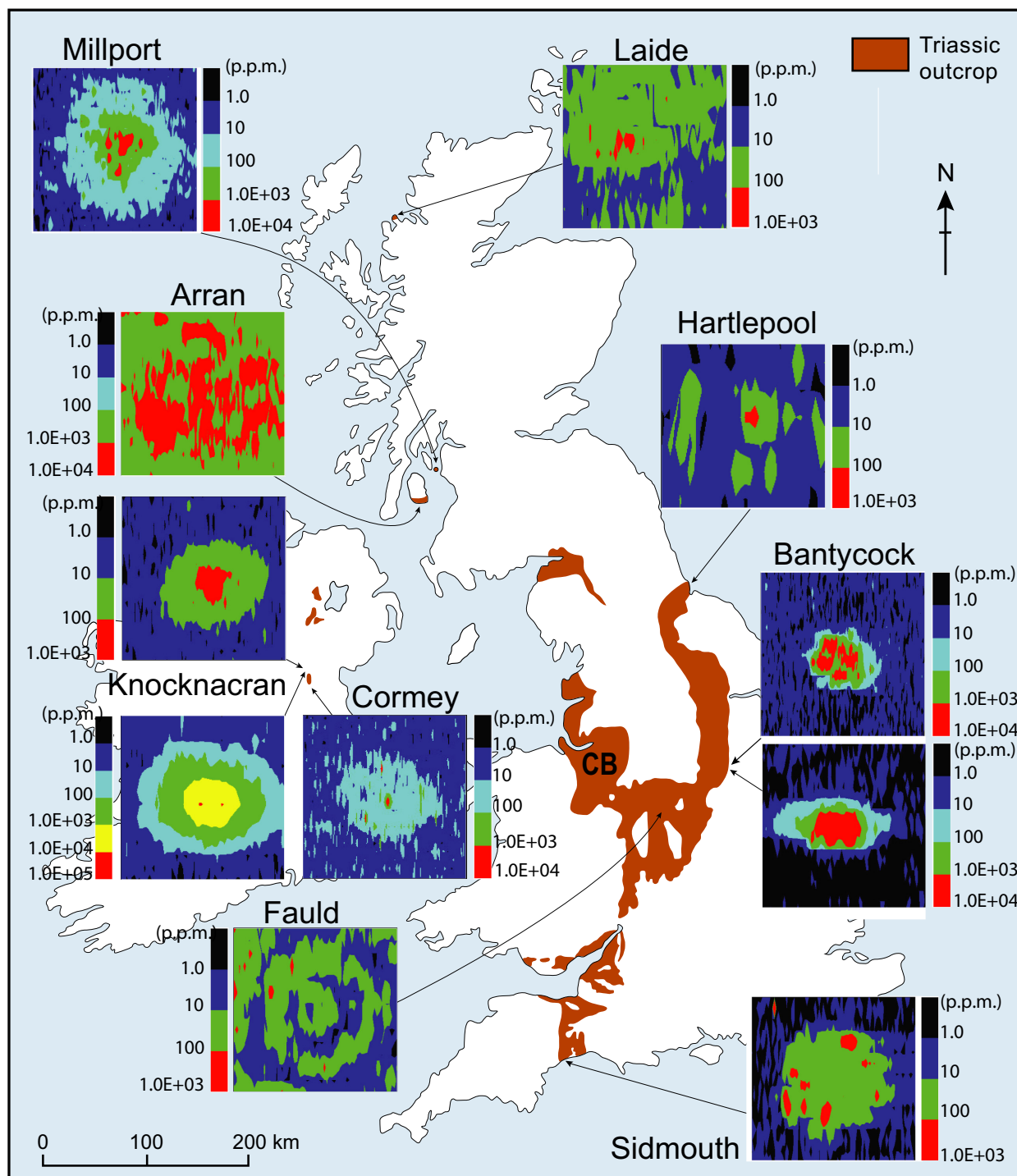


**Fig. 1** LA-ICP-MS maps for Te in reduction spot cores at Triassic sites across the British Isles. Element maps are scaled to show orders of magnitude of concentration in different colours; concentration increases towards the cores of the spheroids. Tellurium enrichment was not recorded at Sidmouth, where a map for Au is shown instead. The tellurium map for the Devonian Millport site is shown for comparison. CB, Cheshire Basin. Maps 3 mm square.

Mo, U and Se, by substituting them for Fe(III) as electron acceptors (Coates *et al.*, 1996; Lovley, 1997). These are all elements concentrated

in red bed deposits, consistent with their purported microbial origin. The elements of interest in this work, Te, Hg and Au, are all also concentrated

from solution by Fe(III)-reducing bacteria (Kashefi *et al.*, 2001; Klonowska *et al.*, 2005; Kerin *et al.*, 2006; Kim *et al.*, 2013), so as these

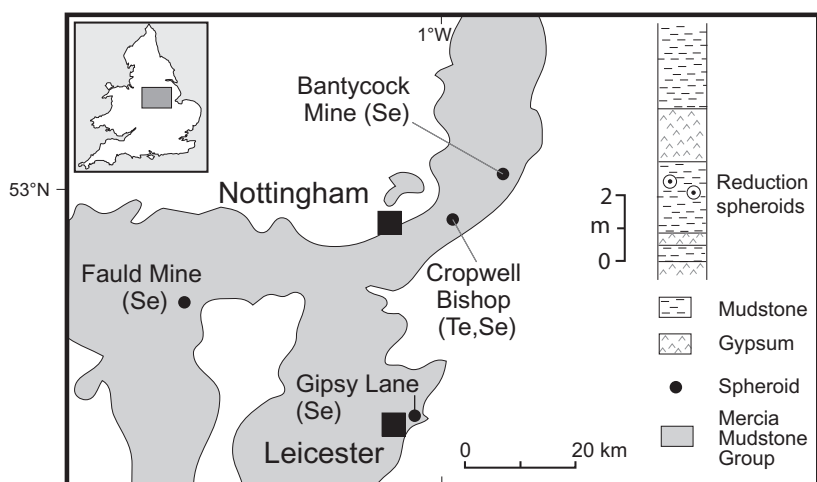


**Fig. 2** Map of the Mercia Mudstone Group in the East Midlands, showing localities sampled for the study of reduction spheroid mineralogy, and indicating whether Te and/or Se were recorded as discrete minerals (clausthalite, kawazulite). Log shows a stratigraphic section for the former gypsum mine at Cropwell Bishop (after Lowe, 1989), indicating the horizon of mudstone containing reduction spheroids from the upper part of the mine.

bacteria will have been abundant in ancient red bed sediments, they are likely to have played a role in Te, Hg and Au concentration.

The occurrence of Se-bearing minerals within several spheroids is comparable with known examples of Se mineralization in other red bed basins, such as in roll-front deposits

(Reynolds and Goldhaber, 1983; Min *et al.*, 2005). This reflects the precipitation of Se under changing redox conditions. The concentration of Se in red beds is favoured by the affinity of Se for iron oxides (Lovley, 1997), which are abundant in red beds. Trace elements in iron oxides are released during recrystallization in

the subsurface (Friedrich and Catalano, 2012; Latta *et al.*, 2012) into potentially mineralizing fluids. The occurrence of Te mineralization in red beds is much less known, reflecting both the low crustal abundance (about 1 p.p.b., Rudnick and Gao, 2003) and its lower mobility in oxidizing environments. However, like Se, Te can be concentrated by an affinity for iron oxides (Harada and Takahashi, 2008).

There is a wider context to the Triassic red bed mineralization reported here. The Triassic Cheshire Basin (Fig. 1), contiguous with our sampling region in the East Midlands, has been exploited for red bed-hosted copper mineralization, in which traces of Au, Hg and Se are recorded (Plant *et al.*, 1999). This is an association comparable with that recorded in the spheroids. The consensus model for mineralization in the Cheshire Basin follows more generalized models for red bed mineralization, in which a reduced sulphur-bearing fluid interacts with an oxidized metal-bearing fluid. In the Cheshire Basin, the Mercia Mudstone Group is proposed as a source of metal-rich fluids derived from iron oxide grain coatings (Plant *et al.*, 1999). This is pertinent because a comparable

**Table 1** Orders of magnitude enrichment of Te and Au in Triassic and other reduction spheroids (background without spheroids, predominant (largest region of map) and maximum values, determined by LA-ICP-MS).

Locality (grid reference)	Age	Te (p.p.m.)			Au (p.p.m.)		
		Background	Predominant	Maximum	Background	Predominant	Maximum
Laide (NG 902925)	Triassic	<1	1–10	100–1000	<1	10–100	10 <sup>4</sup> –10 <sup>5</sup>
Arran (NR 885305)	Triassic	<1	100–1000	10 <sup>3</sup> –10 <sup>4</sup>	<1	1–10	10 <sup>3</sup> –10 <sup>4</sup>
Hartlepool (NZ 525305)	Triassic	<1	1–10	100–1000	<1	1–10	10–100
Knocknacran A (N 805995)	Triassic	1–10	1–10	100–1000	<1	1–10	10–100
Knocknacran B (N 805995)	Triassic	<1 (0.06)*	1–10	10 <sup>4</sup> –10 <sup>5</sup>	<1	1–10	10 <sup>4</sup> –10 <sup>5</sup>
Cormey (N 805975)	Triassic	<1	1–10	10 <sup>3</sup> –10 <sup>4</sup>	<1	1–10	10 <sup>5</sup> –10 <sup>6</sup>
Bantycok A (SK 815495)	Triassic	<1 (0.05)*	1–10	10 <sup>3</sup> –10 <sup>4</sup>	<1	1–10	100–1000
Bantycok B (SK 815495)	Triassic	<1 (0.04)*	1–10	10 <sup>3</sup> –10 <sup>4</sup>	<1	1–10	10–100
Fauld (SK 182283)	Triassic	<1	1–10	100–1000	<1	1–10	100–1000
Sidmouth (SY 131873)	Triassic	<1	1–10	10–100	<1	10–100	100–1000
Culkein (NC 043329)	Proterozoic	<1	1–10	100–1000	<1	1–10	100–1000
Millport (NS 172546)	Devonian	<1 (0.01)*	1–10	10 <sup>3</sup> –10 <sup>4</sup>	<1	1–10	100–1000
Car Rocks (NT 610845)	Carboniferous	<1	10–100	10 <sup>3</sup> –10 <sup>4</sup>	<1	1–10	10 <sup>3</sup> –10 <sup>4</sup>
Cultra (J 403802)	Carboniferous	<1	1–10	100–1000	<1	1–10	10 <sup>3</sup> –10 <sup>4</sup>
Parley's Canyon, Utah, USA	Triassic	<1	1–10	100–1000	<1	1–10	10–100
Kirtomy (NC 742642)*	Devonian	<0.01*	4.50†	–	NA	NA	NA
Budleigh (SY 040803)*	Permian	0.05*	2.40†	–	NA	NA	NA

NA, not analysed.

\*Background values using solution ICP-MS.

†Bulk core values using solution ICP-MS.

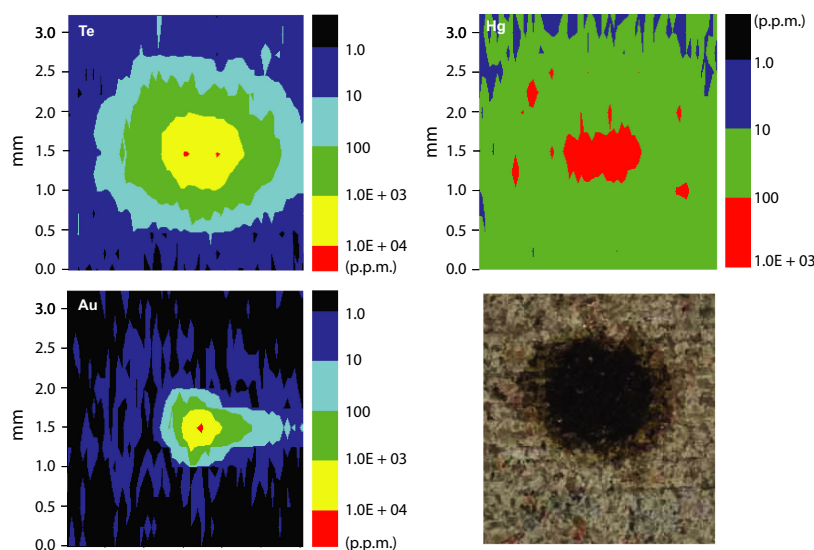


**Fig. 3** Example of a reduction spheroid core in which Te, Hg and Au are co-concentrated. LA-ICP-MS element maps, scaled to show orders of magnitude of concentration in different colours; concentration increases towards the cores of the spheroids. Maps and image of spheroid core 3 mm square. Image shows laser transect lines. Knocknacran, Kingscourt, Ireland.

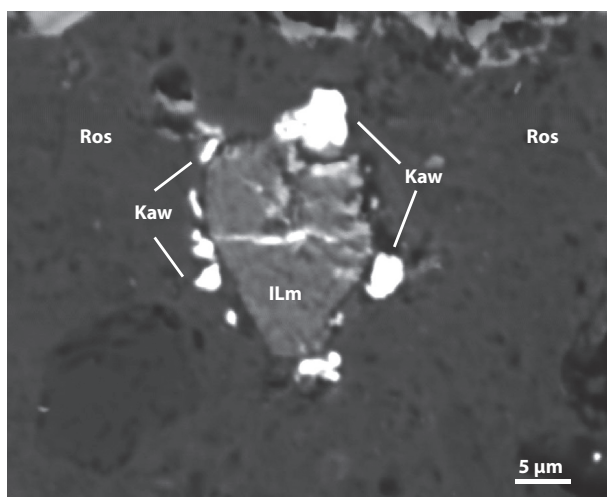


**Fig. 4** Backscattered electron micrograph of the core of a reduction spheroid from Cropwell Bishop, showing crystals of the telluride mineral kawazulite (Kaw) around an ilmenite grain (ILm), in a matrix of the vanadian clay roscelite (Ros).

assemblage of metals is attributed a source in the Mercia Mudstone Group, where the spheroids occur. The spheroids may represent a localized product of the more basin-wide processes that mineralized the Cheshire Basin.

#### Implications for mineralization

The association of Te and Au is typically encountered in magmatic,

metamorphic and hydrothermal deposits (Cook and Ciobanu, 2005; Ciobanu *et al.*, 2006). Similarly, the association of Hg and Au is one normally associated with magmatic systems, metamorphic rocks and placer deposits derived from these rocks (Healy and Petruk, 1990; Naumov and Osovetsky, 2013). The data reported here show that temperature is not a constraint and that where Te and/or Hg are available, regardless

of temperature, Au may be linked to them.

The data for Triassic samples are particularly pertinent to Au mineralization of the sub-Permo-Triassic unconformity in Europe. From the UK to the Czech Republic, Au has precipitated close to the unconformity, interpreted as a redox boundary (Shepherd *et al.*, 2005). The data from numerous Triassic sites indicate that the redox concentration of Au and associated elements is widespread and need not require an exceptional source.

The evidence for a localized enrichment of Te, Hg and Au in the samples from 15 localities over a large area, and also in rocks of different ages, indicates that this may be a normal feature of continental red beds. This knowledge may help develop new strategies to search for Te and Au deposits in continental strata, including the evaluation of roll-front deposits, oil/gas fairways and unconformity surfaces below continental strata, all of which provide redox boundaries where Te and Au could be concentrated.

#### Conclusions

Examination and analysis of the reduction spheroids show that they are consistently enriched in Te, and in some cases also in Hg, Au and Se. The implications of this are as follows:

- (i) Low-temperature Te mobilization may be a normal feature of red bed diagenesis.
- (ii) Te can be concentrated locally in sediments to the point at which discrete Te minerals are precipitated.
- (iii) The Te could be co-concentrated with gold, as in magmatic and metamorphic environments.

#### Acknowledgements

This research was supported by NERC grants (NE/L001764/1, NE/M010953/1). We are grateful to J. Still and A. Sandison for technical support and to the gypsum mines and C. Brolley for access and sampling. Critical comments from Cristiana Ciobanu, Eric Gloaguen and Georges Calas are gratefully acknowledged. The authors have no conflicts of interest to declare.

## References

- Afifi, A.M., Kelly, W.C. and Essene, E.J., 1988. Phase relations among tellurides, sulfides, and oxides: II. Applications to telluride-bearing ore deposits. *Econ. Geol.*, **83**, 395–404.
- Belzile, N. and Chen, Y.W., 2015. Tellurium in the environment: A critical review focused on natural waters, soils, sediments and airborne particles. *Appl. Geochem.*, **63**, 83–92.
- Boyle, R.W., 1979. The geochemistry of gold and its deposits. *Geol. Surv. Can. Bull.*, **280**, 1–584.
- Ciobanu, C.L., Cook, N.J. and Spry, P.G., 2006. Telluride and selenide minerals in gold deposits - how and why? *Mineral. Petrol.*, **87**, 163–169.
- Coates, J.D., Phillips, E.J.P., Lonergan, D.J., Jenter, H. and Lovley, D.R., 1996. Isolation of *Geobacter* species from diverse sedimentary environments. *Appl. Environ. Microbiol.*, **62**, 1531–1536.
- Colman, T.B. and Cooper, D.C., 2000. *Exploration for Metalliferous and Related Minerals in Britain: a Guide*, 2nd edn. British Geological Survey, Keyworth.
- Cook, N.J. and Ciobanu, C.L. 2005. Tellurides in Au deposits: Implications for modelling. In: *Mineral Deposit Research: Meeting the Global Challenge*, Proceedings of the 8th Biennial SGA Meeting, pp. 1387–1390.
- Elliott, R.E., 1961. The stratigraphy of the Keuper Series in Southern Nottinghamshire. *Proc. Yorkshire Geol. Soc.*, **33**, 197–234.
- Friedrich, A.J. and Catalano, J.G., 2012. Controls on Fe(II)-activated trace element release from goethite and hematite. *Environ. Sci. Technol.*, **46**, 1519–1526.
- Harada, T. and Takahashi, Y., 2008. Origin of the difference in the distribution behaviour of tellurium and selenium in a soil-water system. *Geochim. Cosmochim. Acta*, **72**, 1281–1294.
- Harrison, R.K., 1975. Concretionary concentrations of the rarer elements in Permo-Triassic red beds of south-west England. *Geol. Surv. Great Britain Bull.*, **52**, 1–26.
- Healy, R.E. and Petruk, W., 1990. Petrology of Au-Ag-Hg alloy and “invisible” gold in the Trout Lake massive sulfide deposit, Flin Flon, Manitoba. *Can. Mineral.*, **28**, 189–206.
- Hein, J.R., Koschinsky, A. and Halliday, A.N., 2003. Global occurrence of tellurium-rich ferromanganese crusts and a model for the enrichment of tellurium. *Geochim. Cosmochim. Acta*, **67**, 1117–1127.
- Hofmann, B.A., 1990. Reduction spheroids from northern Switzerland: Mineralogy, geochemistry and genetic models. *Chem. Geol.*, **81**, 55–81.
- Kashefi, K., Tor, J.M., Nevin, K.P. and Lovley, D.R., 2001. Reductive precipitation of gold by dissimilatory Fe(III)-reducing bacteria and archaea. *Appl. Environ. Microbiol.*, **67**, 3275–3279.
- Kato, A. 1970. Kawazulite, Bi<sub>2</sub>Te<sub>2</sub>S. In: *Introduction to Japanese Minerals*, pp. 87–88. Geological Survey of Japan, Tokyo, Japan.
- Kerin, E.J., Gilmour, C.C., Roden, E., Suzuki, M.T., Coates, J.D. and Mason, R.P., 2006. Mercury methylation by dissimilatory iron-reducing bacteria. *Appl. Environ. Microbiol.*, **72**, 7919–7921.
- Kilenyi, T. and Standley, R., 1985. Petroleum prospects in the northwest seaboard of Scotland. *Oil Gas J.*, **84**, 100–108.
- Kim, D.H., Kim, M.G., Jiang, S., Lee, J.H. and Hur, H.G., 2013. Promoted reduction of tellurite and formation of extracellular tellurium nanorods by concerted reaction between iron and *Shewanella oneidensis* MR-1. *Environ. Sci. Technol.*, **47**, 8709–8715.
- Klonowska, A., Heulin, T. and Vermiglio, A., 2005. Selenite and tellurite reduction by *Shewanella oneidensis*. *Appl. Environ. Microbiol.*, **71**, 5607–5609.
- Latta, D.E., Gorskil, C.A. and Schere, M.M., 2012. Influence of Fe<sup>2+</sup>-catalysed iron oxide recrystallization on metal cycling. *Biochem. Soc. Trans.*, **40**, 1191–1197.
- Lovley, D.R., 1997. Microbial Fe(III) reduction in subsurface environments. *FEMS Microbiol. Rev.*, **20**, 305–313.
- Lovley, D.R., Chapelle, F.H. and Phillips, E.J.P., 1990. Fe(III)-reducing bacteria in deeply buried sediments of the Atlantic Coastal Plain. *Geology*, **18**, 954–957.
- Lowe, D.J. 1989. Geology of the Cropwell Butler district, 1:10,000 sheet SK 63 NE. Technical Report of the British Geological Survey, Onshore Geology Series, No. WA 89/10.
- McKinley, J.M., Ruffell, A.H. and Worden, R.H., 2012. An integrated stratigraphic, petrophysical, geochemical and geostatistical approach to the understanding of burial diagenesis: Triassic Sherwood Sandstone Group, South Yorkshire, UK. *Int. Assoc. Sedimentol. Spec. Publ.*, **45**, 231–256.
- McNeal, J.M. and Rose, A.W., 1974. The geochemistry of mercury in sedimentary rocks and soils in Pennsylvania. *Geochim. Cosmochim. Acta*, **38**, 1759–1784.
- McPhail, D.C., 1995. Thermodynamic properties of aqueous tellurium species between 25 and 350°C. *Geochim. Cosmochim. Acta*, **59**, 851–866.
- Min, M., Xu, H., Chen, J. and Fayek, M., 2005. Evidence of uranium biomineralization in sandstone-hosted roll-front uranium deposits, northwestern China. *Ore Geol. Rev.*, **26**, 198–206.
- Moss, R.L., Tzimas, E., Kara, H., Willis, P. and Kooroshy, J. 2011. Critical Metals in Strategic Energy Technologies. Assessing Rare Metals as Supply-Chain Bottlenecks in Low-Carbon Energy Technologies. European Commission, Joint Research Centre Institute for Energy and Transport, EUR 24884 EN Report. doi: 10.2790/35600
- Naumov, V.A. and Osovetsky, B.M., 2013. Mercuriferous gold and amalgams in Mesozoic-Cenozoic rocks of the Vyatka-Kama Depression. *Lithol. Min. Resour.*, **48**, 237–253.
- Plant, J.A., Jones, D.G. and Haslam, H.W., eds, 1999. *The Cheshire Basin – Basin Evolution, Fluid Movement and Mineral Resources in a Permo-Triassic Rift Setting*. British Geological Survey, Keyworth.
- Reynolds, R.L. and Goldhaber, M.B., 1983. Iron disulphide minerals and the genesis of roll-type uranium deposits. *Econ. Geol.*, **78**, 105–120.
- Rudnick, R.L. and Gao, S., 2003. Composition of the continental crust. In: *The crust*, Vol. 3 (R.L. Rudnick, ed), 1–64. Elsevier, Amsterdam.
- Schirmer, T., Koschinsky, A. and Bau, M., 2014. The ratio of tellurium and selenium in geological material as a possible paleo-redox proxy. *Chem. Geol.*, **376**, 44–51.
- Shepherd, T.J., Bouch, J.E., Gunn, A.G., McKervey, J.A., Naden, J., Scrivener, R.C., Styles, M.T. and Large, D.E., 2005. Permo-Triassic unconformity-related Au-Pd mineralisation, South Devon, UK: new insights and the European perspective. *Miner. Deposita*, **40**, 24–44.
- Spinks, S.C., Parnell, J. and Bowden, S.A., 2010. Reduction spots in the Mesoproterozoic age: implications for life in the early terrestrial record. *Int. J. Astrobiol.*, **9**, 209–216.
- Spinks, S.C., Parnell, J. and Still, J.W., 2014. Redox-controlled selenide mineralization in the Upper Old Red Sandstone. *Scott. J. Geol.*, **50**, 173–182.
- Spinks, S.C., Parnell, J., Bellis, D. and Still, J., 2016. Remobilization and mineralization of selenium-tellurium in metamorphosed red beds: evidence from the Munster Basin, Ireland. *Ore Geol. Rev.*, **72**, 114–127.
- Turner, R.J., Borghese, R. and Zannoni, D., 2012. Microbial processing of

- tellurium as a tool in biotechnology. *Biotechnol. Adv.*, **30**, 954–963.
- Zepf, V., Reller, A., Rennie, C., Ashfield, M. and Simmons, J., 2014. *Materials Critical to the Energy Industry. An Introduction*, 2nd edn. BP plc, London.
- Zhang, J., Dong, H., Zhao, L., McCarrick, R. and Agrawal, A., 2014. Microbial reduction and precipitation of vanadium by mesophilic and thermophilic methanogens. *Chem. Geol.*, **370**, 29–39.
- Zweibel, K., 2010. The impact of tellurium supply on cadmium telluride photovoltaics. *Science*, **328**, 699–701.
- Received 14 July 2015; revised version accepted 21 March 2016*